

Chapter 5: Synthesis of cobalt imide complexes

The text of this chapter is reproduced in part with permission from:

Jenkins, D. M.; Betley, T. A.; Peters, J. C. *J. Am. Chem. Soc.* **2002**, *124*, 11238-11239.

Copyright 2002 American Chemical Society

5.1 Introduction

Atom- and group-transfer reactions mediated by transition metal centers represent a prominent and heavily scrutinized area of research in inorganic chemistry.¹ Not only are such processes finding relevance in the field of catalysis,² but they have also been proposed in many processes that occur in metalloprotein active sites. First row transition metals that can accept and/or release oxo and nitrene functionalities are particularly interesting.³ For the first row metals Fe, Co, Ni, and Cu, isolable complexes with a terminal imido and/or oxo functionality bonded to a single metal center, $M=E$ or $M\equiv E$ ($E = O, NR$), are rare.⁴ This apparent incompatibility of later metals (groups 9, 10, and 11) with multiply-bonded strong π -donor ligands was overcome in third row transition metal complexes more than 10 years ago (e.g., $[Cp^*]Ir\equiv NR$ and $(Mes_3)Ir\equiv O$).^{5,6} Recently, the quantity of late-metal (group 8 or later) first row transition metal multiple bonds has enjoyed an upsurge, as a number of these complexes have been synthesized. Terminal oxo and nitride complexes have been prepared for iron,⁷ and terminal imido complexes have now been synthesized for iron,^{8,9,10} cobalt,^{10,11,12,13} and nickel.¹⁴ Many of these imido complexes have been reported to undergo reactions wherein the nitrene functionality is transferred to an organic substrate. Two previously described group transfer reactions, which involve loss of the nitrene functionality, include isocyanate production upon addition of CO ^{9,11,15} or aziridination upon addition of olefins.¹⁶

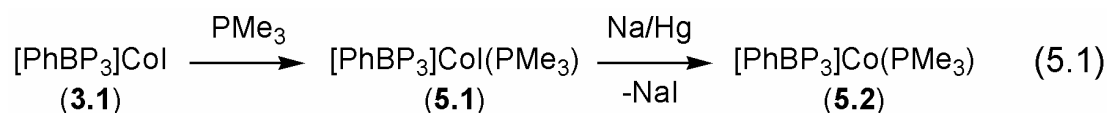
We recently prepared a cobalt(II) complex, $[PhBP_3]CoI$ (**3.1**), exhibiting a distorted tetrahedral geometry and an anomalous low spin ground state.¹⁷ The ground-state electronic configuration proposed for **3.1** (Figure 5.1B) arises from a strong axial distortion of the C_{3v} symmetry, enforced by the geometry of the $[PhBP_3]$ ligand and

In addition to the synthesis and reactivity of these unusual complexes, the electronic structures of these species also are of interest. Theoretical and experimental investigations have been carried out for late-metal third row imides to determine their molecular orbital diagrams, but not for their first row cousins.^{5,18} DFT calculations were performed to shed light on the bonding of the cobalt imide complexes presented here. In addition, species such as isolobal $[\text{PhBP}_3]\text{CoO}$ and $\{[\text{PhBP}_3]\text{CoN}\}^-$ are addressed.

5.2 Results

5.2.1 Synthesis and characterization of precursors $[\text{PhBP}_3]\text{CoI}(\text{PMe}_3)$ and $[\text{PhBP}_3]\text{Co}(\text{PMe}_3)$

The strategy of preparing Co(III) imides from a two-electron oxidation accompanied by azide degradation required the synthesis of a Co(I) reagent. The synthesis of this key Co(I) precursor begins with the synthesis of the red, five-coordinate Co(II) complex, $[\text{PhBP}_3]\text{CoI}(\text{PMe}_3)$ (**5.1**). The addition of neat PMe_3 to a benzene solution of green $[\text{PhBP}_3]\text{CoI}$ (**3.1**) gives **5.1** in quantitative yield (Eq. 5.1). The reduction of **5.1** with a sodium/mercury amalgam produces light green $[\text{PhBP}_3]\text{Co}(\text{PMe}_3)$ (**5.2**) in 90% yield with concurrent loss of NaI .



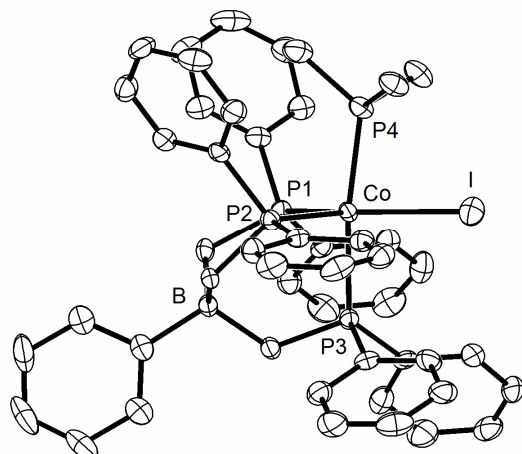


Figure 5.2. Displacement ellipsoids are represented at 50%. Selected interatomic distances (Å) and angles (deg) for [PhBP₃]CoI(PMe₃) (**5.1**): Co-P1, 2.270(1); Co-P2, 2.298(1); Co-P3, 2.353(1); Co-P4, 2.285(1); Co-I, 2.6062(6). P1-Co-P2, 97.72(4); P1-Co-P3, 86.84(4); P2-Co-P3, 89.69(4); P1-Co-P4, 97.42(4); P2-Co-P4, 95.57(4); P3-Co-P4, 172.71(4); P1-Co-I, 137.88(4); P2-Co-I, 124.33(3); P3-Co-I, 90.73(3); P4-Co-I, 82.14(3).

Single crystal X-ray diffraction experiments were undertaken to ascertain the geometry of **5.1** and **5.2**. The distorted trigonal bipyramidal complex [PhBP₃]CoI(PMe₃) has the iodide ligand in the equatorial plane along with two of the three phosphines from the [PhBP₃] ligand (Figure 5.2). Complex **5.1** is structurally very similar to the previously described cationic complex, [(H₃CC(CH₂PPh₂)₃)CoCl(PMe₃)] [BPh₄] (H₃CC(CH₂PPh₂)₃ = triphos).¹⁹

Complex **5.2** has nearly C₃ symmetry in the solid state (Figure 5.3). The Co-P bond distances are all near 2.25 Å, while the P-Co-P bond angles are approximately 92°. The PMe₃ ligand sits on an axial site that shows no off-axis distortion (in **5.2**), with each

of the $P_{[\text{PhBP}_3]}-\text{Co}-P_4$ angles at approximately 124° . The disordered phenyl ring off the boron was refined isotropically in two orientations with the carbon atoms restrained to ideal geometry using isotropic temperature factors and riding hydrogens. Few Co(I) species similar to **5.2** have been structurally characterized. The homoleptic complex $[\text{Co}(\text{PMe}_3)_4][\text{BPh}_4]$ has been prepared and features some distortion of the P-Co-P angles, which range from 101° to 125° .²⁰ The only Co(I) complex supported by a tridentate phosphine is $(\text{np}_3)\text{CoBr}$ ($\text{np}_3 = \text{tris}(2\text{-(diphenylphosphino)ethyl)amine}$), which is a paramagnetic ($S = 1$) species that likewise adopts a pseudotetrahedral geometry. The P-Co-P angles in this case are all near 103° , and the P-Co-Br angles are between 113° and 119° .²¹ The tighter P-Co-P angles for **5.2** are not surprising, given that the ligand is less flexible than np_3 .

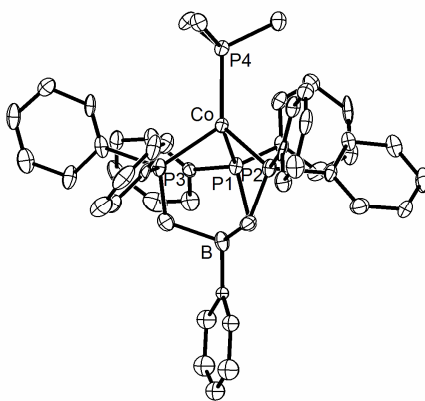


Figure 5.3. Displacement ellipsoids are represented at 50%. The phenyl ring attached to the boron atom in **5.2** is disordered and has been refined isotropically. Selected interatomic distances (\AA) and angles (deg) for $[\text{PhBP}_3]\text{Co}(\text{PMe}_3)$ (**5.2**): Co-P1, 2.244(2); Co-P2, 2.250(2); Co-P3, 2.251(2); Co-P4, 2.305(2); P1-Co-P2, 91.82(7); P1-Co-P3, 91.93(8); P2-Co-P3, 92.31(8); P1-Co-P4, 123.39(8); P2-Co-P4, 124.13(8); P3-Co-P4, 123.95(8).

The magnetism of complexes **5.1** and **5.2** was investigated to determine their ground spin states. Both complexes provide paramagnetic ^1H NMR spectra in C_6D_6 . The solid state magnetization was investigated via SQUID magnetometry; the results are shown in Figure 5.4A. Both complexes obey the Curie-Weiss law, showing spin states of $S = \frac{1}{2}$ for **5.1** ($\chi_m T_{\text{av}}$ (10-300K) = $0.44 \text{ cm}^3 \text{ K mol}^{-1}$) and $S = 1$ for **5.2** ($\chi_m T_{\text{av}}$ (10-300K) = $1.00 \text{ cm}^3 \text{ K mol}^{-1}$). It is not surprising that **5.1** is a low spin species, since phosphine ligands often confer low spin configurations for trigonal bipyramidal Co(II) complexes.²² The Evans's method measurements in C_6D_6 confirm this assignment in solution. The glassy toluene EPR spectra of the complexes are shown in Figure 5.4B. The axial signal ($g_{\parallel} > g_{\perp}$) for complex **5.1** suggests that the trigonal bipyramidal geometry is present in solution as well as the solid state.²³ The combined data show that $[\text{PhBP}_3]\text{CoI}(\text{PMe}_3)$ (**5.1**) has a doublet ground state and that $[\text{PhBP}_3]\text{Co}(\text{PMe}_3)$ (**5.2**) has a triplet ground state. This suggests that the electronic configuration for **5.2** is in accord with the proposed molecular orbital diagram shown in Figure 5.1A.

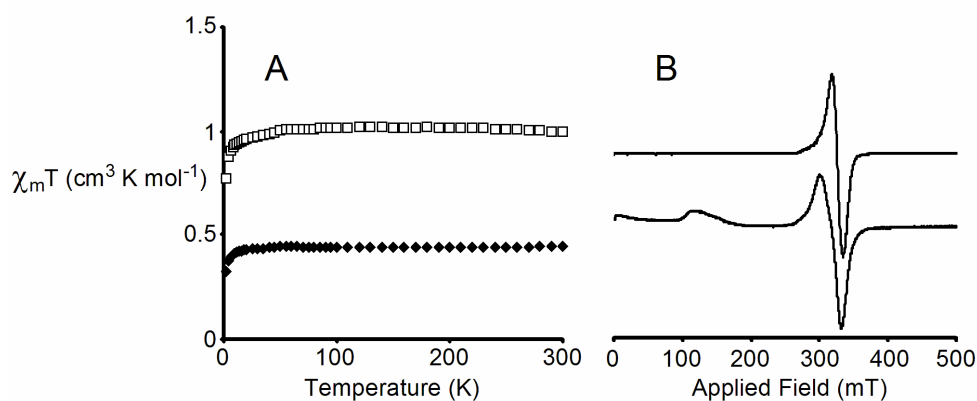
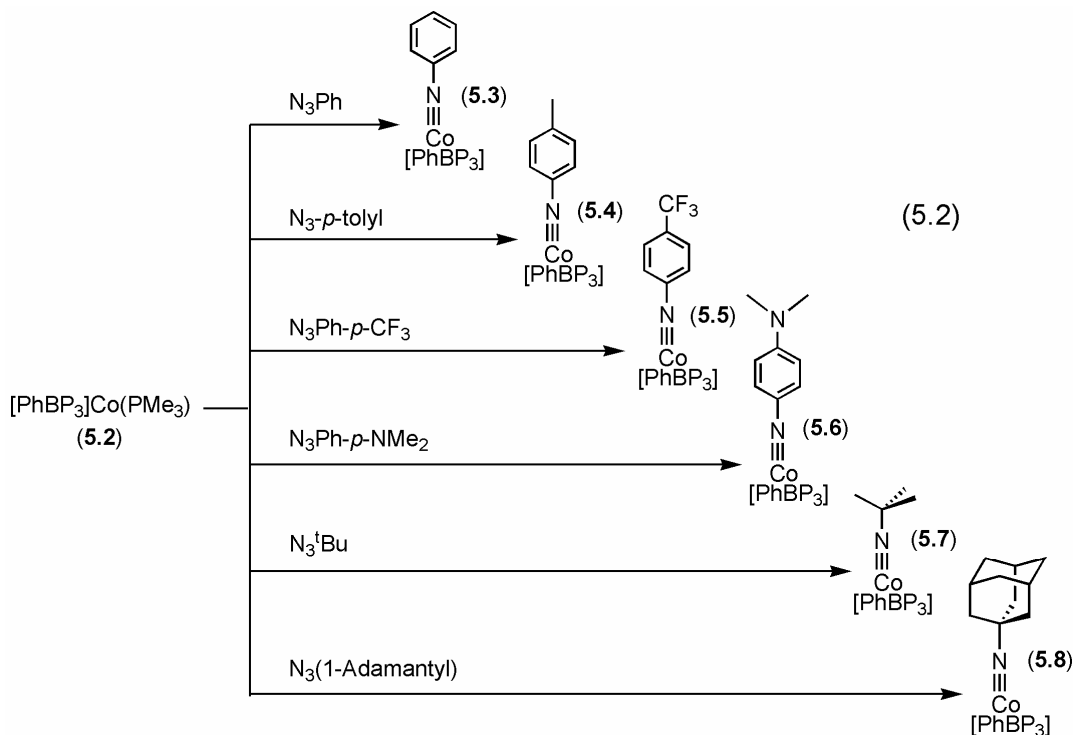


Figure 5.4. (A) SQUID magnetization plot of $\chi_m T$ versus T for $[\text{PhBP}_3]\text{CoI}(\text{PMe}_3)$ (**5.1**), (\blacklozenge) and $[\text{PhBP}_3]\text{Co}(\text{PMe}_3)$ (**5.2**), (\square). (B) EPR spectrum of a glassy toluene solution of **5.1** (top) at 50 K and **5.2** (bottom) at 4 K.

5.2.2 Synthesis of imido complexes via azide reduction

A variety of Co(III) imides can be generated from $[\text{PhBP}_3]\text{Co}(\text{PMe}_3)$, **5.2**. The addition of two equivalents of an arylazide, such as phenylazide, to a benzene solution of **5.2** gives rise to a bright red solution (Eq. 5.2). In addition to the desired imide, $[\text{PhBP}_3]\text{CoNPh}$ (**5.3**), the byproducts $\text{Me}_3\text{P}=\text{NPh}$ and N_2 are also formed. The iminophosphorane can be removed by washing the solids with petroleum ether or through crystallization from benzene and petroleum ether. The reaction has proven general for a number of different arylazides with either electron withdrawing and electron donating groups on the aryl ring. Three additional arylimido complexes were synthesized with this methodology, including $[\text{PhBP}_3]\text{CoN-}p\text{-tolyl}$ (**5.4**), $[\text{PhBP}_3]\text{CoN}(4\text{-CF}_3\text{-Ph})$ (**5.5**), and $[\text{PhBP}_3]\text{CoN}(4\text{-NMe}_2\text{-Ph})$ (**5.6**). All four species are diamagnetic and show one broad resonance in the ^{31}P NMR around 68 ppm. The ^1H NMR of the species also suggests that they have C_3 symmetry in solution at ambient temperature.

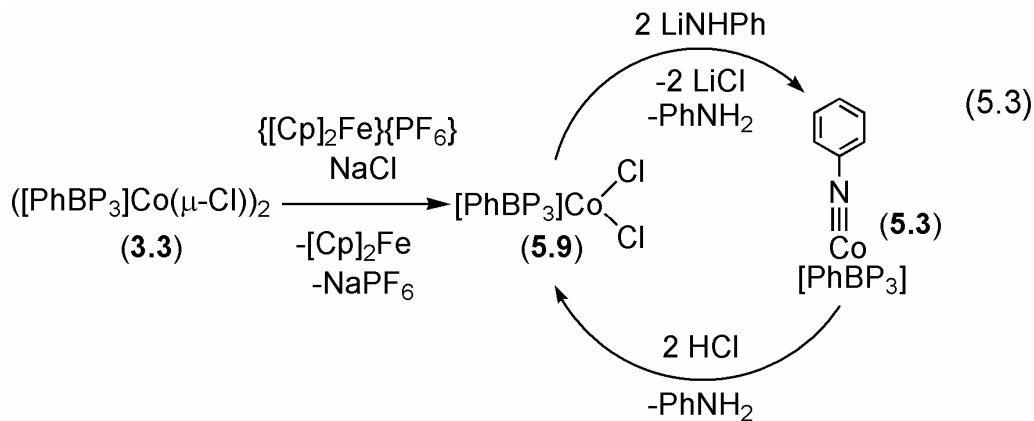


The synthesis of imides from $[\text{PhBP}_3]\text{CoPMe}_3$ (**5.2**) and alkylazides is also feasible, although the reactions are slower than with the arylazides. For example, the reaction between **5.2** and N_3^tBu requires heating at $55\text{ }^\circ\text{C}$ for several hours to be driven to completion. Two alkylimide complexes were prepared from **5.2** and their corresponding azides, $[\text{PhBP}_3]\text{CoN}^t\text{Bu}$ (**5.7**) and $[\text{PhBP}_3]\text{CoNAd}$ (**5.8**) (Ad = 1-adamantyl) (Eq. 5.2). These species are diamagnetic and show similar ^1H and ^{31}P NMR spectra to the arylimide complexes. The bright red color of the arylimido complexes, presumably arising from a ligand-to-metal charge transfer band, is not present in the alkylimide complexes. None of the Co(III) imides feature a reversible oxidation or reduction in a cyclic voltammogram between $+600\text{ mV}$ to -2000 mV versus ferrocenium. On the other hand, the iron imides prepared in our laboratory, such as $[\text{PhBP}_3]\text{FeNAd}$, which can be reduced to its Fe(II) anion $\{[\text{PhBP}_3]\text{FeNAd}\}^-$.²⁴

5.2.3 Synthesis of imides via metathesis

Although aryl or alkylazides allow for the synthesis of the Co(III) imide complexes beginning with a Co(I) precursor, we were interested in extending the methodology to more conventional routes. Bergman's iridium imide, $[\text{Cp}^*]\text{IrN}^t\text{Bu}$, is synthesized via metathesis using $([\text{Cp}^*]\text{IrCl}_2)_2$ and four equivalents of LiNH^tBu . Likewise, Hillhouse has prepared a three-coordinate nickel(II) imide using amide metathesis followed by oxidation and deprotonation. To evaluate whether a dehydrohalogenation route would work with our system, we needed to synthesize an appropriate Co(III) starting material that would be isoelectronic to $[\text{Cp}^*]\text{IrCl}_2$. The cyclic voltammogram for **3.1** showed a reversible $\text{Co}^{\text{II/III}}$ oxidative wave at 10 mV versus ferrocene/ferrocenium, while the chloride derivative $([\text{PhBP}_3]\text{Co}(\mu\text{-Cl}))_2$ (**3.3**) showed

the same oxidative wave at -80 mV. Since **3.3** is a monomer in solution, this result suggested that **3.3** could be cleanly oxidized using a ferrocenium salt. Addition of excess solid NaCl to a THF solution of **3.3** in the presence of a stoichiometric quantity of $\{[\text{Cp}]_2\text{Fe}\}\{\text{PF}_6\}$ gave the green diamagnetic complex $[\text{PhBP}_3]\text{CoCl}_2$ (**5.9**) (Eq. 5.3). Complex **5.9** is a five-coordinate complex that has a distorted square pyramidal geometry as can be seen in the solid-state structure in Figure 5.5. The two *trans* angles for P-Co-Cl are both greater than 154° . This complex is structurally analogous to $[(\text{triphos})\text{CoCl}_2][\text{BF}_4]$ prepared by Huttner and co-workers. Interestingly, this five-coordinate complex **5.9** has only a single ^{31}P NMR resonance at 36 ppm suggesting that the phosphorous atoms exchange positions rapidly on the NMR time scale.



The addition of two equivalents of PhNHLi to a benzene solution of **5.9** immediately causes the reaction mixture to turn red (Eq. 5.3). After purification, the only cobalt product present was identified as $[\text{PhBP}_3]\text{CoNPh}$ (**5.3**) by comparing its ^1H NMR, ^{31}P NMR, and UV-vis spectra to that of **5.3** prepared by the synthetic route described above. No cobalt amide species is detected, even when a less than one equivalent of PhNHLi is used. ^{31}P NMR shows only the starting material, $[\text{PhBP}_3]\text{CoCl}_2$ (**5.9**), and the

imide, **5.3**. Conversion of the imide (**5.3**) to the Co(III) dichloride (**5.9**) is also feasible.

Addition of two equivalents of HCl in ether to $[\text{PhBP}_3]\text{CoNPh}$ gives $[\text{PhBP}_3]\text{CoCl}_2$.

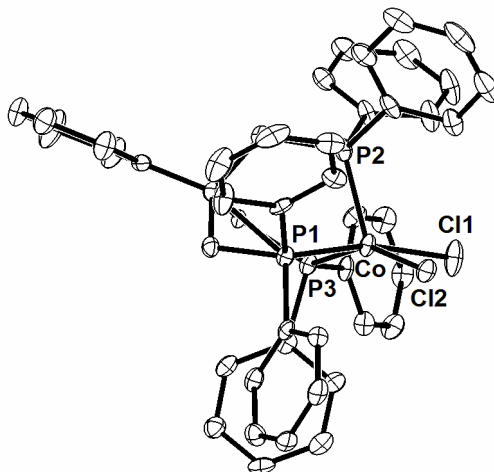


Figure 5.5. Displacement ellipsoids are represented at 50%. Selected interatomic distances (Å) and angles (deg) for $[\text{PhBP}_3]\text{CoCl}_2$ (**5.9**): Co-P1, 2.268(1); Co-P2, 2.182(1); Co-P3, 2.235(1); Co-Cl1, 2.226(1); Co-Cl2, 2.210(1). P1-Co-P2, 89.77(5); P1-Co-P3, 93.88(4); P2-Co-P3, 88.35(4); Cl1-Co-P1, 165.47(5); Cl1-Co-P2, 104.60(5); Cl1-Co-P3, 88.75(4); Cl2-Co-P1, 84.18(4); Cl2-Co-P2, 117.34(5); Cl2-Co-P3, 154.18(5); Cl1-Co1-Cl2, 87.24(4).

5.2.4 Structural characterization of the Co(III) imides

The structural parameters of two of the cobalt imides were established by single crystal X-ray diffraction. The solid state structures of $[\text{PhBP}_3]\text{CoN-}p\text{-tolyl}$ (**5.4**) and $[\text{PhBP}_3]\text{CoN}^t\text{Bu}$ (**5.7**) are shown in Figure 5.6 and Figure 5.7, respectively. The structure of **5.4** shows a slight distortion from C_3 symmetry; the P-Co-N bond angles vary from 115° to 132° . The short Co-N distance of 1.658(2) Å and the nearly linear Co-N-C(46)

angle of $169.51(2)^\circ$ suggest a triple bond as shown in Figure 5.1C. Complex **5.7** has even less distortion from C_3 symmetry, since the variance between the P-Co-N angles in this case is less than five degrees, between 122° and 126° . Likewise, the Co-N-C46 angle is more linear at $176.68(13)^\circ$ and the Co-N bond length is slightly shorter at $1.633(2)$. These Co-N bond distances are slightly longer than the reported distance of the β -diketiminato supported imide $[\text{HC}(\text{CMeNC}_6\text{H}_3\text{-2,6-Me}_2)_2]\text{CoNAd}$ ($[\text{HC}(\text{CMeNC}_6\text{H}_3\text{-2,6-Me}_2)_2]^- = [\text{Me}_2\text{NN}]$), which is $1.624(4)$ Å. Furthermore, the Co-N-C bond angle for the planar species $[\text{Me}_2\text{NN}]\text{CoNAd}$ is slightly more bent at $161.5(3)^\circ$ than these $[\text{PhBP}_3]$ supported imides. Another Co(III) imide prepared in our laboratory, $[\text{PhBP}^{i\text{Pr}}_3]\text{CoN-}p\text{-tolyl}$ ($[\text{PhBP}^{i\text{Pr}}_3] = [\text{PhB}(\text{CH}_2\text{P}^i\text{Pr}_2)_3]^-$), features a similar Co-N bond distance ($1.667(2)$ Å) and Co-N-C bond angle ($173.2(2)^\circ$). More recently, a cationic cobalt(III) imide supported by a neutral tridentate N-heterocyclic carbene ligand has been reported by Meyer and co-workers. The geometry is best described as pseudotetrahedral, and the Co-N bond distance ($1.675(2)$ Å) is only slightly longer than the distances for our cobalt imides. This arylimide complex has Co-N-C bond angle ($168.6(2)^\circ$) that is very close to the bond angle of **5.4**. Late-metal four-coordinate iron imides feature Fe-N bond lengths and Fe-N-C bond angles that are close to the cobalt imides we have structurally characterized.^{8,9}

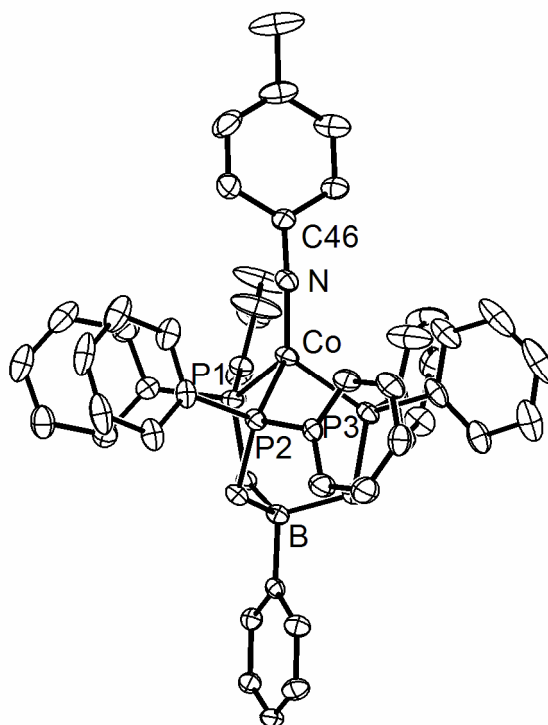


Figure 5.6. Displacement ellipsoids are represented at 50%. Selected interatomic distances (Å) and angles (deg) for [PhBP₃]CoN-*p*-tolyl (**5.4**): Co-N, 1.658(2); N-C46, 1.370(2); Co-P1, 2.1719(6); Co-P2, 2.1892(6); Co-P3, 2.1618(6). P1-Co-P2, 93.13(2); P1-Co-P3, 89.07(2); P2-Co-P3, 91.24(2); P1-Co-N, 115.32(6); P2-Co-N, 131.89(6); P3-Co-N, 125.64(6) Co-N-C46, 169.51(2).

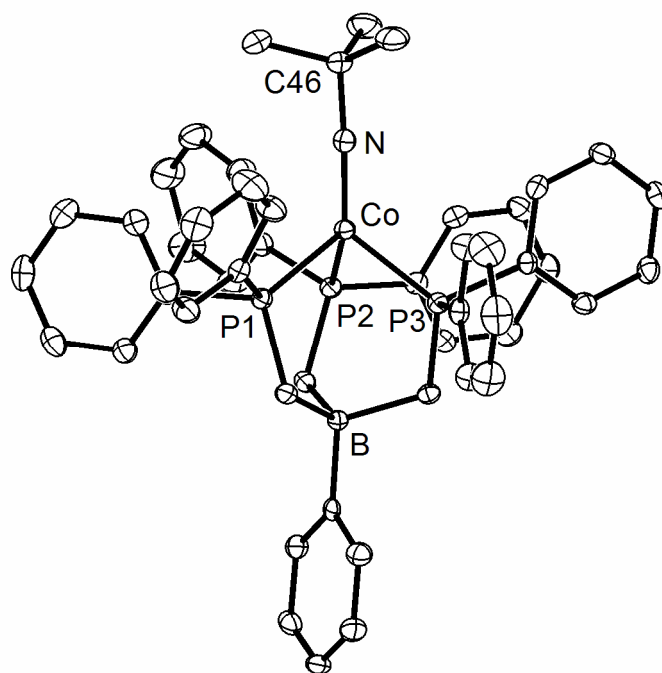
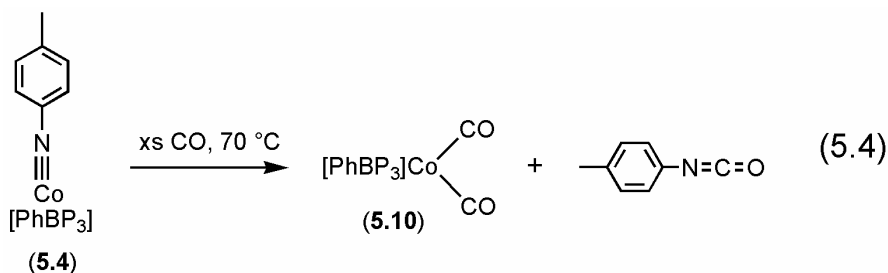


Figure 5.7. Displacement ellipsoids are represented at 50%. Selected interatomic distances (Å) and angles (deg) for [PhBP₃]CoN^tBu (**5.7**): Co-N, 1.633(2); N-C46, 1.441(2); Co-P1, 2.1595(5); Co-P3, 2.1765(5); Co-P2, 2.1823(5). P1-Co-P2, 91.46(2); P1-Co-P3, 92.18(2); P2-Co-P3, 88.95(2); N-Co-P1, 122.24(5); N-Co-P2, 125.24(5); N-Co-P3, 126.49(5).

5.2.5 Reactivity of the Co(III) imide complexes

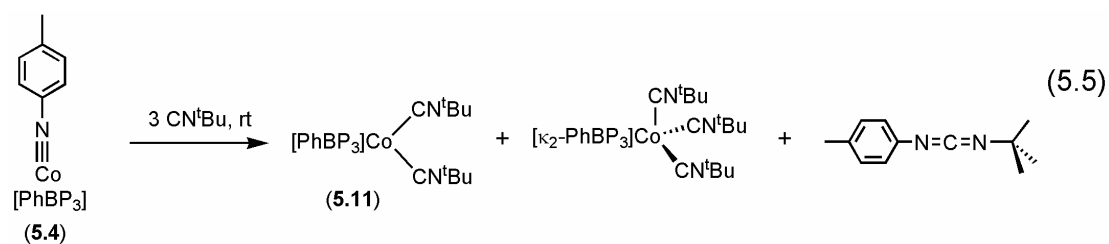
A catalytic cycle wherein the imide is formed from an organic azide and from which the nitrene functional group could be transferred to an organic compound would be a valuable synthetic tool. Ideally, aziridination could be achieved using these aryl or alkylazides and olefins. Previous examples of aziridination were only successful with tosylazide²⁵ or, more commonly, the hypervalent iodide reagent PhI=NTs

(Ts = -S(O)₂-*p*-tolyl).²⁶ Notably, Hillhouse and co-workers have been able to perform an aziridination reaction from an isolated Ni imide complex, (dtbpe)NiN(2,6-di-isopropylphenyl) (dtbpe = 1,2-bis(di-*tert*-butylphosphino)ethane), and ethylene, although they were unable to prepare the imide species from azide degradation. Even with prolonged heating, we have been unable to cause the nitrene functionality from **5.4** to react with an olefin (such as styrene) to give an aziridine (such as 1-*p*-tolyl-2-phenyl-cyclopropane). We have had greater success inducing reactivity between the imide complexes and π -acids. For example, we find that the imido functionality can be transferred slowly from **5.4** to carbon monoxide to produce the isocyanate (O=C=N-*p*-tolyl) (14 equiv of CO, 70 °C, 12 days). The isolated cobalt(I) byproduct (90%) was the diamagnetic dicarbonyl species [PhBP₃]Co(CO)₂ (**5.10**) (Eq. 5.4). This contrasts to the behavior of Bergman's imide, [Cp*]IrN^tBu, which reacts with CO but does not give the free isocyanate.^{5a} Despite attempts to turn over a catalytic cycle, we have been unable to provoke additional azide to react with [PhBP₃]Co(CO)₂ to form an imide complex and additional isocyanate. This lack of reactivity of the Co(I) dicarbonyl contrasts with a similar species we have prepared in our laboratory, [PhBP₃]Fe(CO)₂, which reacts with *p*-tolylazide to give the imide complex and *p*-tolyl-isocyanate.



Addition of three equivalents of *tert*-butylisocyanide to **5.4** at ambient temperature gives the mixed carbodiimide *p*-tolyl-N=C=N-^tBu as the organic product

(Eq. 5.5). More than one metal-containing byproduct was detected in this reaction, and an independent synthesis of $[\text{PhBP}_3]\text{Co}(\text{CN}^t\text{Bu})_2$ (**5.11**) from $[\text{PhBP}_3]\text{CoI}(\text{CN}^t\text{Bu})$ (**5.12**), CN^tBu , and Na/Hg amalgam (see Experimental Section for details) confirmed this species to be one of the two metal-containing products. Two additional peaks in the ^{31}P NMR of the reaction mixture in a ratio of 2:1 suggest that the other metal-containing product is most likely diamagnetic $[\kappa_2\text{-PhBP}_3]\text{Co}(\text{CN}^t\text{Bu})_3$, whose synthesis we have yet to independently realize, even by addition of excess CN^tBu to $[\text{PhBP}_3]\text{Co}(\text{CN}^t\text{Bu})_2$ (**5.11**). The only reported example of this type of reaction on late metal imides involves an iridium imide complex in which the carbodiimide is not released from the metal center.^{5a}



Unlike the related $[\text{PhBP}_3]\text{FeN-}p\text{-tolyl}$, which releases aniline as a product when exposed to H_2 , none of the cobalt imides we have examined react with H_2 .²⁷ The stability of the complexes is also manifested in their lack of reactivity with oxygen and water; only after prolonged exposure do they degrade. Furthermore, the imides are thermally robust, as **5.4** can be heated for days to 100° in toluene with only modest decomposition.

5.3 Discussion

Due to the unusual nature of this metal-ligand multiple bond, the orbital splitting diagram of these imide species is of interest. The molecular orbital diagrams of late third row transition metal imide bonds have received attention in the past. Bergman suggests that up to d^6 imides would be stable supposing that the d_z^2 orbital does not interact too

strongly with the auxiliary ligand, in his case [Cp*].^{5a} Photoelectron spectroscopy studies provided experimental support for this assertion. The suggested d orbital splitting diagram included a low-lying non-bonding e set followed by an a_1 orbital and a high-lying π -antibonding e set. On the basis of our recent EPR studies of [PhBP₃]FeN-*p*-tolyl, it seemed possible that the ground state configuration could best be described as $(d_z^2)^2(d_{x^2-y^2})^2(d_{xy})^1(d_{xz})^0(d_{yz})^0$ for a d^5 imide species. To evaluate whether this was a good model of the cobalt imide complexes, DFT calculations were performed using the X-ray structure of **5.7** as a starting point. In light of the approximate C_{3v} symmetry that this complex adopts, one would expect the d -orbitals to transform into two e sets (xy , x^2-y^2 and xz , yz) and one a_1 set (d_z^2) as shown in Figure 5.1C. A large HOMO-LUMO is predicted by this model.

The results of the DFT energy minimization and orbital calculation are shown in Figure 5.8. The calculated geometry is in excellent agreement with the experimental geometry, excluding an elongation of each of the Co-P bonds by 0.08 Å. Two ligand-based orbitals (MO 206 and 209) are interspersed near the five d orbitals and involve C-C π -bonds on the phenyl ring attached to the boron. The orbital of a_1 symmetry is the lowest in energy, approximately 6 kcal/mol lower than the non-bonding e set (xy , x^2-y^2). The higher lying e set (xz , yz) shows strong π -antibonding with the nitrogen, again suggesting a stable triple bond. The large HOMO-LUMO gap, calculated at 91 kcal/mol, is responsible for the stabilization of the metal-ligand multiple bond species, as the π^* orbitals are empty. Similar results were obtained from a DFT study of **5.4**. The molecular orbital splitting diagram is reminiscent of the molecular orbital diagram of d^6 sandwich complexes such as [Cp]₂Fe or {[Cp]₂Co}⁺.²⁸

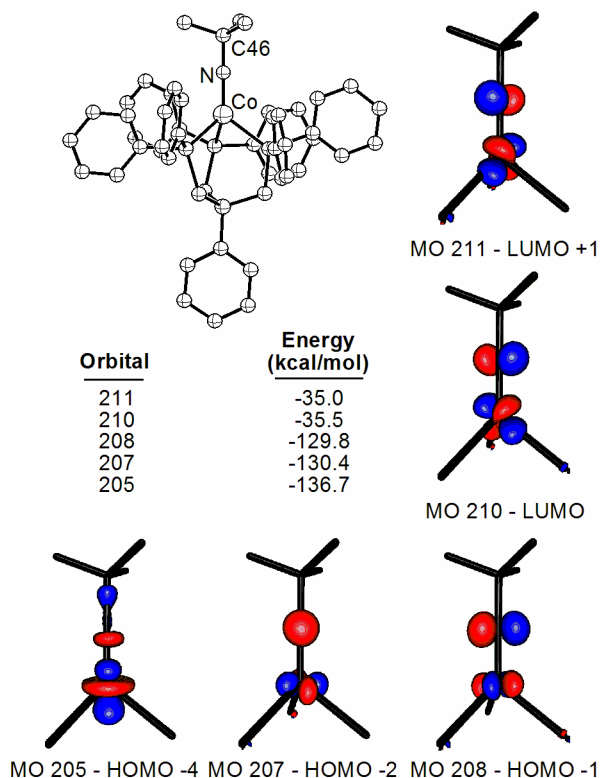


Figure 5.8. Molecular orbitals derived from a DFT energy minimization of $[\text{PhBP}_3]\text{CoN}^t\text{Bu}$ (5.7) assuming a singlet ground state and the crystallographically determined atomic coordinates as a starting point.

These cobalt(III) imides feature stable cobalt-nitrogen triple bonds in agreement with their symmetry and molecular orbital diagram. The d^6 configuration was shown to be stable for a pseudotetrahedral imide over a decade ago by Bergman. What is perhaps more intriguing is the question of why unsubstituted multiply bonded ligands, such as $[\text{PhBP}_3]\text{Co}\equiv\text{O}$, are not stable in this d^6 configuration. The only example of a group 9 or later terminal heteroatom metal-ligand multiple bond remains the d^4 iridium oxo $(\text{Mes})_3\text{Ir}\equiv\text{O}$ (Mes = mesityl) prepared by Wilkinson over a decade ago.^{6,29} We propose that the predicted stability of metal-ligand multiple bonds can only be addressed by dividing these species into two classes: terminal, with no additional atoms attached to

multiply bonded ligands (e.g., oxos and nitrides), and non-terminal, with additional atoms attached to multiply bonded ligands (e.g., imidos).

The stability of the two classes is more subtle than can be predicted using a back-of-the-envelope molecular orbital diagram. The nature of the sigma bond between the metal and the ligand must be taken into account. More specifically, the amount of mixing between the p_z and d_z^2 orbitals on the metal and between the p_z and s orbitals on the heteroatom ligand is critical. The d_z^2 orbital is shown in Figure 5.9 for three calculated complexes: $[\text{PhBP}_3]\text{CoN}^t\text{Bu}$ (**5.7**) and the hypothetical molecules $[\text{PhBP}_3]\text{CoNH}$ and $\{[\text{PhBP}_3]\text{CoN}\}^-$. Owing to its attenuated HOMO-LUMO gap, which arises from the terminally bonded nitride ligand, we anticipate that $\{[\text{PhBP}_3]\text{CoN}\}^-$ to be electronically less stable than $[\text{PhBP}_3]\text{CoN}^t\text{Bu}$. The hypothetical cobalt nitride features strong σ -antibonding with the cobalt d_z^2 and the p_z on the nitrogen. This is consistent with a complex synthesized in our laboratory, the d^4 nitride $[\text{PhBP}^{i\text{Pr}}_3]\text{Fe}\equiv\text{N}$,^{7a} and suggests that the lone pair on the nitrogen atom has an almost fully s orbital character. Oxidizing the species by two electrons would remove electrons from this antibonding orbital.

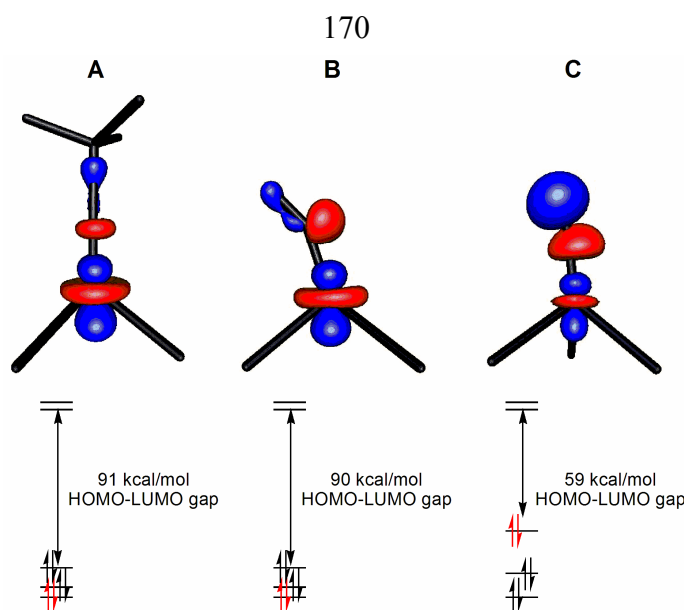


Figure 5.9. Molecular orbital diagrams derived from DFT calculations of $[\text{PhBP}_3]\text{CoN}^t\text{Bu}$ (A), $[\text{PhBP}_3]\text{CoNH}$ (B), and $\{[\text{PhBP}_3]\text{CoN}\}^-$ (C). Only the central atoms are shown for clarity. The orbital representations show the d_z^2 for each molecule, and its position of the molecular orbital diagram is depicted by the red electrons.

Alternatively, substituted multiply bonded ligand allows the lone pair on the heteroatom to hybridize to an sp configuration, which lowers the energy of the d_z^2 orbital. Due to the destabilization at the terminal atom, it would seem difficult to stabilize a metal-ligand multiple bond for a terminal atom in a tetrahedral d^6 configuration. More generally, if a late-metal metal-ligand multiple bond for a non-terminal atom is stable for a d^n electron configuration, a terminal atom should only be stable with a d^{n-2} electron configuration. This hypothesis is supported not only by work performed in our laboratory on cobalt and iron, but also by others working in this field. Presently, we have been unable to synthesize a terminal nitride or oxo of Co(III) , but the imides are readily accessible. The related $[\text{PhBP}_3]\text{Fe}$ and $[\text{PhBP}^{i\text{Pr}}_3]\text{Fe}$ systems support up to d^6 imides,¹ but

only a d^4 nitride.^{7a} Likewise, Hillhouse and co-workers have reported a d^8 imide complex in a trigonal planar geometry, but no corresponding terminal atom metal-ligand multiple bond such as an oxo. This hypothesis does not suggest that the terminal metal-ligand multiple bond is thermodynamically preferred over a bridging species, such as a μ_2 -nitride versus a terminal nitride. Warren and co-workers prepared a trigonal planar Co(III) imide featuring an adamantyl group off of the nitrogen, but using smaller substituents such as 3,5-dimethylphenyl formed a bridging bis- μ_2 -imide.^{12,30} Obviously, this hypothesis only holds if the complexes being compared are of the same geometry.

Our attempts to prepare a $[\text{PhBP}_3]\text{Co}\equiv\text{O}$ have failed primarily due to the destabilization of terminal atoms versus non-terminal atoms for a d^6 pseudotetrahedral complex. The Co(III) siloxide $\{[\text{PhBP}_3]\text{CoOSiPh}_3\}\{\text{BAr}_4\}$ (**4.15**) $\{\text{BAr}_4\}$ (Ar = Ph, or 3,5-(CF₃)₂-C₆H₃) is relatively stable, but under no conditions have we been able to remove the silyl group to form $[\text{PhBP}_3]\text{Co}\equiv\text{O}$, even though this species is isolobal to the stable imides we have prepared.³¹ Likewise, a comparison of the d_z^2 orbitals from **4.15** to the theoretically calculated $[\text{PhBP}_3]\text{CoO}$ show the same effect as the imide versus nitride (Figure 5.10). In fact, the DFT results for **4.15** suggest that this complex has a molecular orbital diagram similar to the imides but with somewhat weaker π -bonding. In addition to strong σ -antibonding from the d_z^2 orbital, the hypothetical oxo $[\text{PhBP}_3]\text{CoO}$ is off-axis like the calculated nitride $\{[\text{PhBP}_3]\text{CoN}\}^-$. This model predicts that in a pseudotetrahedral geometry only a d^4 oxo or nitride such as $\{[\text{PhBP}_3]\text{CoN}\}^+$ would be stable.

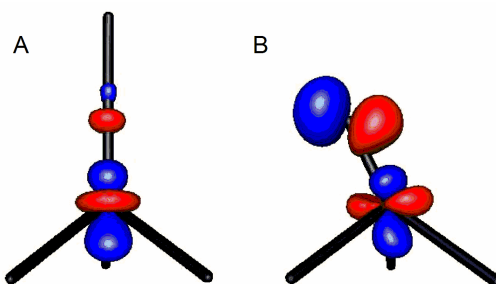


Figure 5.10. Orbital representations showing the d_z^2 orbital: (A) $\{[\text{PhBP}_3]\text{CoOSiPh}_3\}^+$ (**4.15**) and (B) $[\text{PhBP}_3]\text{CoO}$. Only the central atoms are shown for clarity.

The second fundamental shift in metal-ligand bonds lies in the nature of the R group on the imido nitrogen. More subtly, the parent imide $[\text{PhBP}_3]\text{CoNH}$ is less stable than $[\text{PhBP}_3]\text{CoN}^t\text{Bu}$ (Figure 5.9). While the strong σ -antibonding interaction is not apparent, as in the case of the nitride complex, and the HOMO-LUMO gap is almost as large, the position of the calculated imide does not sit in the axial position, as it has nearly formed an equatorial plane with two of the phosphines. This result suggests that the hybridization on the N-H bond is not as effective as an N-C bond at attenuating the σ -antibonding interaction with the d_z^2 orbital. The NH group is being moved away from the σ -antibonding d_z^2 orbital, suggesting that dimeric NH imides may be electronically favored. To date, efforts to synthesize the parent imide $[\text{PhBP}_3]\text{CoNH}$ have been unsuccessful. Although bulky substituents on the imide nitrogen, such as a *tert*-butyl group, can favor the formation of terminal imides over other products, particularly bridging imides, it seems likely that the NH fragment is not as favorable electronically as other groups.³² While it is impossible to separate the steric and electronic issues fully, it

is worth noting that the number of structurally characterized $M\equiv NH$ imide complexes is far smaller than the number of $M\equiv NR$ ($R = \text{alkyl or aryl}$) imide species that have been reported.³³ At present, no structurally characterized example of a terminal $M\equiv NH$ has been reported for an electron count greater than d^3 , while $M\equiv NR$ imides have now been synthesized with electron counts as high as d^8 .³⁴

The inertness of the Co(III) imides ultimately rests on their electronic stability as closed shell 18 electron species. Saturated imides with a large HOMO-LUMO gap are resistant to giving up the nitrene functionality in group transfer reactions. This explains why this system is so inert, both to air and water, as well as chemical transformations. Comparable imide complexes, such as $[\text{PhBP}_3]\text{FeNPh}$ ^{9,24,27} and Hillhouse's nickel imide,^{14,15,16} are unsaturated species (with 17 and 16 electrons, respectively), which helps explain their greater reactivity. In light of the molecular orbital diagram for the cobalt imide species, it is not surprising that they undergo very few reactions.

5.4 Conclusions

We have synthesized the first imides on cobalt and they are supported by the $[\text{PhBP}_3]$ auxiliary ligand. Their synthesis can be adapted either from oxidative degradation of azides with a cobalt(I) precursor or salt metathesis of lithium amides with a Co(III) dihalide complex. The imides only react to give up the nitrene functionality in the case of CO or CN^tBu addition, giving the isocyanate and the carbodiimide as organic by-products respectively. The electronic structure diagram of the imides is similar to the well-known molecular orbital diagram for $\{[\text{Cp}]_2\text{Co}\}^+$ or $[\text{Cp}]_2\text{Fe}$ as well as their third row relative, $[\text{Cp}^*]\text{IrN}^t\text{Bu}$. These pseudotetrahedral species confirm that the $[\text{PhBP}_3]\text{Co}\equiv\text{ER}$ species effectively have an *octahedral* molecular orbital diagram.

5.5 Experimental section

5.5.1 General considerations

General procedures were performed according to Section 2.4.1 and 3.5.1. Magnetic measurements were conducted as described in Section 3.5.2. EPR measurements and simulations were conducted as described in Section 3.5.3.

5.5.2 EPR measurements

Instrumental parameters for the spectra shown:

For [PhBP₃]CoI(PMe₃) (**5.1**) in Figure 5.2: EPR spectrum of a glassy toluene solution of [PhBP₃]CoI(PMe₃) at 50 K. Instrumental parameters: $\nu = 9.621$ GHz, modulation frequency = 100 KHz, modulation amplitude = 2 G, microwave power = 2.017 mW, conversion time = 20.48 ms, time constant = 5.12 ms, 10 scans.

For [PhBP₃]Co(PMe₃) (**5.2**) in Figure 5.2: EPR spectrum of a glassy toluene solution of [PhBP₃]Co(PMe₃) at 4 K. Instrumental parameters: $\nu = 9.476$ GHz, modulation frequency = 100 kHz, modulation amplitude = 15 G, microwave power = 2.01 mW, conversion time = 81.92 ms, time constant = 20.48 ms, 5 scans.

5.5.3 DFT calculations

All calculations were performed using the hybrid DFT functional B3LYP as implemented in the Jaguar 5.0 program package.³⁵ This DFT functional utilizes the Becke three-parameter functional³⁶ (B3) combined with the correlation functional of Lee, Yang, and Parr³⁷ (LYP). LACVP** was used as the basis set. Input coordinates were derived as described in the text from crystallographically determined structures (**5.4**, **5.7**, and **4.15** {BPh₄}). The starting structures of [PhBP₃]CoNH and {[PhBP₃]CoN}⁻ used the framework of **5.7** subtracting the *tert*-butyl group off the imide and adding a hydrogen

atom at a reasonable distance in the case of [PhBP₃]CoNH. The starting structure of [PhBP₃]CoO used the framework of {**4.15**} removing the silyl group. Spin-states and molecular charges were explicitly stated, and no molecular symmetry was imposed. Default values for geometry and SCF iteration cutoffs were used. All structures converged under these criteria.

5.5.4 Starting materials and reagents

The reagents CN^tBu, NaCl, {[Cp]₂Fe}{PF₆}, 1-azidoadamantane (1-adamantylazide), PMe₃, CO, 1.0 M HCl in Et₂O, sodium, and mercury metal were purchased from commercial vendors and used without further purification. PhNHLi was freshly prepared by addition of 1 equiv. of 1.6 M BuLi to 1 equiv. of PhNH₂ in petroleum ether. The resulting precipitate was collected via vacuum filtration and washed with additional petroleum ether. The reagents N₃Ph,³⁸ N₃-*p*-tolyl, N₃Ph-*p*-CF₃,³⁹ N₃Ph-*p*-NMe₂,⁴⁰ and N₃^tBu⁴¹ were prepared according to literature procedures. The preparation of [PhBP₃]CoI (**3.1**) and ([PhBP₃]Co(μ-Cl))₂ (**3.3**) is described in Chapter 3. The preparation of {[PhBP₃]CoOSiPh₃}{BAR₄} ({**4.15**}{BAR₄} Ar = Ph or 3,5-(CF₃)₂-C₆H₃) is described in Chapter 4.

5.5.5 Synthesis of compounds

Synthesis of [PhBP₃]CoI(PMe₃), 5.1. Neat PMe₃ (34 μL, 0.32 mmol) was added via microsyringe to a stirring solution of [PhBP₃]CoI (**3.1**) (0.254 g, 0.291 mmol) in benzene (10 mL). The initially green solution turned red instantly. After stirring for 15 min, the solution was frozen, and the benzene was removed by lyophilization to afford a pure red powder (0.272 g, 99 % yield). Crystals were grown via vapor diffusion of petroleum ether into a benzene solution. ¹H NMR (C₆D₆, 300 MHz): δ 22.6 (br), 10.8, 9.4 (br), 7.4

(m), 2.2, 1.2 (m). UV-vis (C_6H_6) λ_{max} , nm (ϵ): 472 (1700). Anal. Calcd for $C_{48}H_{50}BICoP_4$: C, 60.85; H, 5.32. Found: C, 60.88; H, 5.11.

Synthesis of [PhBP₃]Co(PMe₃), 5.2: A 0.71 % Na/Hg amalgam was prepared by dissolving 7.3 mg (0.32 mmol) of sodium in 1.03 g of mercury. A THF solution (12 mL) of [PhBP₃]CoI(PMe₃) (**5.1**) (0.272 g, 0.29 mmol) was added to the stirring amalgam suspension in THF (5 mL). The mixture was stirred for 6 h as the color changed from red to brown. The heterogeneous reaction mixture was filtered through Celite to remove the amalgam, and the filtrate was dried in vacuo to a fine brown powder. The brown powder was then dissolved in 15 mL of benzene and stirred vigorously. After 1 h, a white precipitate (NaI) was observed, which was removed by filtration through Celite. The brown filtrate was frozen and dried to a fine brown powder by lyophilization (0.212 g, 90% yield). The product is extremely air sensitive and can be recrystallized via vapor diffusion of petroleum ether into benzene to give light green crystals. ¹H NMR (C_6D_6 , 300 MHz): δ 42 (br), 15.8, 14.9, 13.2, 8.4, 8.2, 7.4 (m), 1.2 (m), -3.2, -3.6, -7.2 (br). UV-vis (C_6H_6) λ_{max} , nm (ϵ): 680 (140). Anal. Calcd for $C_{48}H_{50}BCoP_4$: C, 70.26; H, 6.14. Found: C, 70.17; H, 6.11.

Synthesis of [PhBP₃]CoNPh, 5.3. A benzene (2 mL) solution of phenylazide (39.2 mg, 0.329 mmol) was added dropwise to a stirring benzene (10 mL) solution of [PhBP₃]Co(PMe₃) (**5.2**) (135 mg, 0.164 mmol). During the first 15 min, nitrogen evolution was evident, and the brown solution turned deep red. The solution was stirred for an additional 4 h to ensure completion. The solvent was removed by lyophilization. The resulting red powder was washed with petroleum ether (10 mL) to remove the byproduct (Me₃P=NPh) and then dried to afford pure product (104 mg, 76%). The product can be recrystallized via vapor diffusion of petroleum ether into benzene. ¹H NMR (C₆D₆, 300 MHz): δ 8.191 (d, *J* = 7.8 Hz, 2 H), 8.129 (d, *J* = 7.2 Hz, 2 H), 7.735 (m, 14 H), 7.492 (t, *J* = 7.2 Hz, 1 H), 7.348 (t, *J* = 7.5 Hz, 1 H), 7.059 (t, *J* = 7.5 Hz, 2 H), 6.731 (m, 18 H), 1.481 (br, 6 H). ³¹P NMR (C₆D₆, 121.4 MHz): δ 69 (br). ESI/MS (*m/z*): 836 (**5.3** + H⁺). UV-vis (C₆H₆) λ_{max}, nm (ε): 418 (7000), 538 (4200). Anal. Calcd for C₅₁H₄₆BCoNP₃: C, 73.31; H, 5.55; N, 1.68. Found: C, 72.35; H, 5.43; N, 1.87.

Synthesis of [PhBP₃]CoN-*p*-tolyl, 5.4. A benzene (2 mL) solution of *p*-tolylazide (50.6 mg, 0.380 mmol) was added dropwise to a stirring benzene (10 mL) solution of [PhBP₃]Co(PMe₃) (**5.2**) (156 mg, 0.190 mmol). During the first 15 min, nitrogen evolution was evident, and the brown solution turned deep red. The solution was stirred for an additional 4 h to ensure completion. The solvent was removed by lyophilization. The resulting red powder was washed with petroleum ether (10 mL) to remove the byproduct (Me₃P=N-*p*-tolyl) and then dried to afford pure product (157 mg, 97%). The product can be recrystallized via vapor diffusion of petroleum ether into benzene. ¹H NMR (C₆D₆, 300 MHz): δ 8.141 (d, *J* = 7.2 Hz, 2 H), 7.764 (m, 14 H), 7.494 (t, *J* = 7.5 Hz, 1 H), 6.857 (d, *J* = 8.1 Hz, 2 H), 6.749 (m, 20 H), 1.769 (3 H), 1.491 (br, 6 H). ³¹P

NMR (C_6D_6 , 121.4 MHz): δ 69 (br). ^{13}C NMR (C_6D_6 , 209.5 MHz): δ 138.6, 134.6, 132.6, 131.7, 129.0, 128.9, 128.5, 128.3, 128.2, 125.0, 120.4, 22.7, 12.7 (br). ESI/MS (m/z): 850 (**5.4** + H^+). UV-vis (C_6H_6) λ_{max} , nm (ϵ): 420 (5700), 536 (3400). Anal. Calcd for $C_{52}H_{48}BCoNP_3$: C, 73.51; H, 5.69; N, 1.65. Found: C, 73.64; H, 5.61; N, 1.63.

Synthesis of [PhBP₃]CoNPh-*p*-CF₃, 5.5. A benzene (2 mL) solution of $N_3Ph-p-CF_3$ (95.8 mg, 0.512 mmol) was added to a stirring benzene (10 mL) solution of [PhBP₃]Co(PMe₃), **5.2**, (210 mg, 0.256 mmol). The reaction mixture was stirred for 5 h at rt and then frozen and dried to a dark red powder by lyophilization. The powder was washed with acetonitrile (2 x 15 mL) and dried affording the product (139 mg, 60% yield). 1H NMR (C_6D_6 , 300 MHz): δ 8.11 (d, $J = 7.2$ Hz, 2 H), 7.92 (d, $J = 7.8$ Hz, 2 H), 7.73 (t, $J = 7.5$ Hz, 2 H), 7.66 (m, 12 H), 7.48 (t, $J = 7.2$ Hz, 1 H), 7.23 (d, $J = 8.1$ Hz, 2 H), 6.75 (m, 18 H), 1.46 (br s, 6 H). $^{31}P\{^1H\}$ NMR (C_6D_6 , 121.4 MHz): δ 65 (br). ^{19}F NMR (C_6D_6 , 282 MHz): -61.2. UV-vis (C_6H_6) λ_{max} , nm (ϵ): 422 (6800), 549 (4500). Anal. Calcd for $C_{52}H_{45}BCoF_3NP_3$: C, 69.12; H, 5.02; N, 1.55. Found: C, 68.72; H, 5.41; N, 1.55.

Synthesis of [PhBP₃]CoNPh-*p*-NMe₂, 5.6. A benzene (2 mL) solution of $N_3Ph-p-NMe_2$ (31.0 mg, 0.191 mmol) was added to a stirring benzene (5 mL) solution of [PhBP₃]Co(PMe₃), **5.2**, (78.4 mg, 0.096 mmol). The reaction mixture was stirred for 8 h at rt and then frozen and dried to a dark red powder by lyophilization. The powder was washed with petroleum ether (2 x 10 mL), dried, and then dissolved in benzene (2 mL). Crystallization via vapor diffusion of petroleum ether into the benzene solution yielded pure product (52 mg, 62% yield). 1H NMR (C_6D_6 , 300 MHz): δ 8.04 (d, $J = 8.4$ Hz, 2 H), 8.17 (d, $J = 6.9$ Hz, 2 H), 7.84 (m, 12 H), 7.74 (t, $J = 6.9$ Hz, 2 H), 7.49 (t, $J = 6.6$ Hz, 1

H), 6.78 (m, 18 H), 6.34 (d, $J = 8.4$ Hz, 2 H), 2.33 (s, 6 H), 1.54 (br s, 6 H). $^{31}\text{P}\{^1\text{H}\}$ NMR (C_6D_6 , 121.4 MHz): δ 64 (br). UV-vis (C_6H_6) λ_{max} , nm (ϵ): 454 (10500), 543 (9900). Anal. Calcd for $\text{C}_{53}\text{H}_{51}\text{BCoN}_2\text{P}_3$: C, 72.45; H, 5.85; N, 3.19. Found: C, 72.10; H, 5.98; N, 3.07.

Synthesis of [PhBP₃]CoN^tBu, 5.7. A benzene (2 mL) solution of N_3^tBu (114 mg, 1.16 mmol) was added to a stirring benzene (8 mL) solution of [PhBP₃]Co(PMe₃), **5.2**, (159 mg, 0.194 mmol). The reaction mixture was stirred and heated to 55° C for 6 h. After cooling to rt, the reaction mixture was frozen and dried to a brown powder by lyophilization. This powder was then washed with petroleum ether (2 x 10 mL) and dried to afford the product (41 mg, 26% yield). The product can be crystallized via vapor diffusion of petroleum ether into benzene. ^1H NMR (C_6D_6 , 300 MHz): δ 8.12 (d, $J = 6.9$ Hz, 2 H), 7.70 (t, $J = 7.8$ Hz, 2 H), 7.66 (m, 12 H), 7.46 (t, $J = 7.2$ Hz, 1 H), 6.78 (m, 18 H), 1.58 (s, 9 H), 1.49 (br s, 6 H). $^{31}\text{P}\{^1\text{H}\}$ NMR (C_6D_6 , 121.4 MHz): δ 70 (br). UV-vis (C_6H_6) λ_{max} , nm (ϵ): 480 (1500).

Synthesis of [PhBP₃]CoNAd, 5.8. A benzene (5 mL) solution of 1-azidoadamantane (177 mg, 1.00 mmol) was added to a stirring benzene (7 mL) solution of [PhBP₃]Co(PMe₃), **5.2**, (205 mg, 0.250 mmol). The reaction mixture was stirred for 2 h at rt and then frozen and dried to a brown powder by lyophilization. The powder was washed with petroleum ether (2 x 10 mL), dried, then washed with acetonitrile (2 x 10 mL), and dried to afford the product (100 mg, 45% yield). ^1H NMR (C_6D_6 , 300 MHz): δ 8.13 (d, $J = 7.2$ Hz, 2 H), 7.73 (m, 12 H), 7.71 (t, $J = 7.8$ Hz, 2 H), 7.47 (t, $J = 7.2$ Hz, 1 H), 6.80 (m, 18 H), 2.36 (s, 6 H), 1.99 (s, 3 H), 1.71 (s, 6 H), 1.51 (br s, 6 H). $^{31}\text{P}\{^1\text{H}\}$ NMR (C_6D_6 , 121.4 MHz): δ 70 (br). UV-vis (C_6H_6) λ_{max} , nm (ϵ): 479 (1400). Anal.

Calcd for $C_{55}H_{56}BCoNP_3$: C, 73.92; H, 6.32; N, 1.57. Found: C, 73.57; H, 6.46; N, 1.77.

Synthesis of $[PhBP_3]CoCl_2$, **5.9.** A THF (80 mL) solution of $([PhBP_3]Co(\mu-Cl))_2$, **3.3**, (0.936 g, 0.600 mmol) was stirred vigorously prior to addition of solid $\{[Cp]_2Fe\}\{PF_6\}$ (0.437 g, 0.132 mmol). The solution immediately turned bright green. After 5 min, solid NaCl (0.701 g, 1.20 mmol) was added to the solution, which was then stirred for 16 h. The reaction mixture was then filtered through Celite, and the filtrate was dried in vacuo affording a fine green powder. The powder was washed with petroleum ether (3 x 75 mL) to remove $[Cp]_2Fe$. The green powder was dissolved in benzene (150 mL) and was stirred vigorously for 6 h followed by filtration through Celite. The green filtrate was then frozen and dried to an analytically pure powder by lyophilization (0.594 g, 61% yield). The product can be crystallized via vapor diffusion of petroleum ether into benzene. 1H NMR (C_6D_6 , 300 MHz): δ 7.91 (d, $J = 6.9$ Hz, 2 H), 7.73 (m, 12 H), 7.62 (t, $J = 6.9$ Hz, 2 H), 7.42 (m, 1 H), 6.84 (m, 6 H), 6.68 (m, 12 H), 1.39 (s br, 6 H). $^{31}P\{^1H\}$ NMR (C_6D_6 , 121.4 MHz): δ 36. UV-vis (C_6H_6) λ_{max} , nm (ϵ): 484 (690), 645 (750). Anal. Calcd for $C_{45}H_{41}BCl_2CoP_3$: C, 66.29; H, 5.07. Found: C, 66.42; H, 4.85.

Alternative synthesis of $[PhBP_3]CoNPh$, **5.3.** A benzene (10 mL) solution of $[PhBP_3]CoCl_2$, **5.9**, (223 mg, 0.273 mmol) was added to a stirring slurry of PhNHLi (54.2 mg, 0.547 mmol) in benzene (5 mL). The reaction mixture changed from green to red and was stirred for 2 h followed by filtration over Celite. The red filtrate was frozen and dried by lyophilization and then washed with petroleum ether (2 x 10 mL). The red powder was then dried in vacuo (120 mg, 53% yield). Spectroscopic methods indicated that the product was pure **5.3** showing identical UV-vis, ^{31}P NMR, and 1H NMR signals.

Alternative synthesis of [PhBP₃]CoCl₂, 5.9. A diethyl ether (15 mL) solution of [PhBP₃]CoNPh, **5.3**, (82 mg, 0.098 mmol) was stirred vigorously prior to addition of 1.0 M HCl in diethyl ether (196 μ L, 0.196 mmol) via micropipette. The reaction mixture immediately changed from red to green and solids precipitated. The reaction mixture was filtered over Celite, and benzene (2 x 10 mL) was used to extract more product from the Celite. The green filtrate was then frozen and dried to a powder by lyophilization and then washed with petroleum ether (2 x 5 mL) and dried in vacuo (32 mg, 40% yield). Spectroscopic methods indicated that the product was pure **5.9** showing identical UV-vis, ³¹P NMR, and ¹H NMR signals.

Synthesis of [PhBP₃]Co(CO)₂, 5.10. An atmosphere of CO was added to a 200 mL Strauss flask that contained a benzene (8 mL) solution of [PhBP₃]CoN-*p*-tolyl (**5.4**) (25.4 mg, 0.030 mmol). The flask was heated to 70 °C in an oil bath for 8 d during which the color changed from deep red to light brown. GC/MS of the reaction mixture showed the formation of phenylisocyanate (*m/z* = 119). The solution was then frozen, and the solvent was removed by lyophilization. The resulting tan powder was washed with petroleum ether (10 mL) and then dried to afford pure product (22 mg, 90 %). ¹H NMR (C₆D₆, 300 MHz): δ 8.084 (d, *J* = 7.2 Hz, 2 H), 7.667 (t, *J* = 7.2 Hz, 2 H), 7.433 (t, *J* = 7.2 Hz, 1 H), 7.377 (m, 12 H), 6.783 (m, 18 H), 1.781 (br s, 6 H). ³¹P NMR (C₆D₆, 121.4 MHz): δ 35.5. ¹³C NMR (C₆D₆, 125.7 MHz): δ 211.1, 139.3, 133.3, 131.6, 130.6, 129.9, 129.1, 124.2, 16.7 (br). IR (cm⁻¹, THF): 2008, 1932. UV-vis (C₆H₆) λ_{max} , nm (ϵ): 440 (880). Anal. Calcd for C₄₇H₄₁BCoO₂P₃: C, 70.52; H, 5.16. Found: C, 70.90; H, 5.27.

Synthesis of [PhBP₃]Co(CN^tBu)₂, 5.11. A 0.61% Na/Hg amalgam was prepared by dissolving 3.3 mg (0.14 mmol) of sodium into 540 mg of mercury. A THF (10 mL)

solution of $[\text{PhBP}_3]\text{CoI}(\text{CN}^t\text{Bu})$, **5.12** (see below), (136 mg, 0.14 mmol) was added to the stirring amalgam in THF (3 mL). Neat CN^tBu (12 mg, 0.14 mmol, 16 μL) was then added via micropipette. The mixture was stirred for 3 h as the color changed from green to brown. The reaction mixture was then filtered through Celite to remove the amalgam, and the filtrate was dried in vacuo affording a fine brown powder. The brown powder was dissolved in benzene (12 mL) and stirred vigorously. After 1 h, white precipitate (NaI) was observed, which was removed by filtration through Celite. The orange filtrate was frozen and dried to a fine orange powder through lyophilization (129 mg, 100% yield). ^1H NMR (C_6D_6 , 300 MHz): δ 8.12 (d, $J = 6.3$ Hz, 2 H), 7.63 (t, $J = 7.5$ Hz, 2 H), 7.58 (m, 12 H), 7.39 (t, $J = 6.3$ Hz, 1 H), 6.88 (m, 18 H), 1.75 (s, 6 H), 1.06 (s, 18 H). $^{31}\text{P}\{^1\text{H}\}$ NMR (C_6D_6 , 121.4 MHz): δ 39. IR (cm^{-1} , THF): 2113, 2040. Anal. Calcd for $\text{C}_{55}\text{H}_{59}\text{BCoN}_2\text{P}_3$: C, 72.53; H, 6.53; N, 3.08. Found: C, 72.48; H, 6.92; N, 3.01.

Synthesis of $[\text{PhBP}_3]\text{CoI}(\text{CN}^t\text{Bu})$, **5.12.** A benzene (2 mL) solution of CN^tBu (23.2 mg, 0.279 mmol) was added to a stirring benzene (10 mL) solution of $[\text{PhBP}_3]\text{CoI}$, **3.1**, (243 mg, 0.279 mmol). The reaction mixture was stirred for 10 h at rt and then frozen and dried to a green powder by lyophilization. The powder was washed with petroleum ether (2 x 15 mL) and dried affording the product (237 mg, 89% yield). ^1H NMR (C_6D_6 , 300 MHz): δ 10.6 (br), 7.9, 7.7, 7.4, 7.3, 7.0, 2.9 (br). UV-vis (C_6H_6) λ_{max} , nm : 423 (2400), 701 (1100). Anal. Calcd for $\text{C}_{50}\text{H}_{50}\text{BCoINP}_3$: C, 62.92; H, 5.28; N, 1.47. Found: C, 62.76; H, 5.44; N, 1.23.

Addition of CO to $[\text{PhBP}_3]\text{CoN-}p\text{-tolyl}$ (5.4**).** To a J. Young tube was added **5.4** (12.7 mg, 0.015 mmol) and ferrocene (2.0 mg) as an internal standard in C_6D_6 . The tube was then charged with CO (14 equiv, 0.210 mmol). The J. Young tube was heated for 12 days

at 70 °C in an oil bath. A ^1H NMR spectrum of the reaction mixture was compared to a pure sample of *p*-tolylisocyanate, confirming only 30% of the free isocyanate by integration (GC/MS: 133 *m/z* for *p*-tolylisocyanate). An additional peak in the alkyl region (45% by integration) suggested another product(s), presumably due to isocyanate degradation during the course of the experiment. Only free isocyanate was detected by GC/MS.

Addition of CN^tBu to $[\text{PhBP}_3]\text{CoN-}p\text{-tolyl}$ (5.4**).** Neat CN^tBu (27.6 mg, 0.333 mmol, 37.7 μL) was added via micropipette to a stirring solution of $[\text{PhBP}_3]\text{CoN-}p\text{-tolyl}$, **5.4**, (94.1 mg, 0.111 mmol) in benzene (8 mL) at ambient temperature. The reaction mixture went from red to brown over 6 h. The solution was frozen and dried to a fine brown powder through lyophilization. The powder was washed with petroleum ether (2 x 10 mL). The petroleum ether fraction was set aside to settle and decanted 30 min later and dried in vacuo. The powder fraction was dried in vacuo. Organic products from the petroleum ether fraction were characterized by GC/MS, which showed $^t\text{BuN}=\text{C}=\text{NPh-}p\text{-CH}_3$. GC/MS (*m/z*): 188 (M), 132 (M- ^tBu). Inorganic products from the solid showed $[\text{PhBP}_3]\text{Co}(\text{CN}^t\text{Bu})_2$, **5.11**, (by IR, ^{31}P NMR and ^1H NMR) as well as an additional product tentatively assigned as $\kappa_2\text{-}[\text{PhBP}_3]\text{Co}(\text{CN}^t\text{Bu})_3$. $^{31}\text{P}\{^1\text{H}\}$ NMR (C_6D_6 , 121.4 MHz): δ 45 (2 P), 9 (1 P). IR (cm^{-1} , THF): 2142 (additional peaks may be obscured by overlapping **5.11**).

5.5.6 X-ray experimental information

The general X-ray experimental procedure was performed according to section 2.4.4. Crystallographic information is provided in Table 5.1.

Table 5.1. X-ray diffraction experimental details for [PhBP₃]CoI(PMe₃) (**5.1**), [PhBP₃]Co(PMe₃) (**5.2**), [PhBP₃]CoN-*p*-tolyl (**5.4**), [PhBP₃]CoN^tBu (**5.7**), and [PhBP₃]CoCl₂ (**5.9**).

	[PhBP ₃]CoI(PMe ₃), (5.1)	[PhBP ₃]Co(PMe ₃), (5.2)
Chemical formula	C ₅₄ H ₅₆ BCoIP ₄	C ₄₈ H ₅₀ BP ₄ Co · C ₆ H ₆
Formula weight	1025.51	898.61
T (°C)	-177	-177
λ (Å)	0.71073	0.71073
a (Å)	19.1690(9)	13.204(2)
b (Å)	12.2981(6)	13.313(2)
c (Å)	21.3027(10)	17.112(3)
α (°)	90	72.299(2)
β (°)	105.5100(10)	88.479(2)
γ (°)	90	60.454(2)
V (Å ³)	4839.1(4)	2465.2(7)
Space group	P2 ₁ /c	P $\bar{1}$
Z	4	2
D _{calcd} (g/cm ³)	1.408	1.211
μ (cm ⁻¹)	11.61	5.12
R1, wR2 (I > 2σ(I)) ^a	0.0580, 0.1099	0.1044, 0.1820

$$^a R1 = \frac{\sum ||F_o| - |F_c||}{\sum |F_o|}, wR2 = \left\{ \frac{\sum [w(F_o^2 - F_c^2)^2]}{\sum [w(F_o^2)^2]} \right\}^{1/2}$$

Table 5.1. (cont.)

	[PhBP ₃]CoN- <i>p</i> -tolyl (5.4)	[PhBP ₃]CoN ^t Bu (5.7)
Chemical formula	C ₅₅ H ₅₁ BCoNP ₃	C ₄₉ H ₅₀ BNP ₃ Co · 1½(C ₆ H ₆)
Formula weight	888.62	932.71
T (°C)	-177	-177
λ (Å)	0.71073	0.71073
a (Å)	14.1174(11)	11.2939(5)
b (Å)	14.3252(11)	18.4709(8)
c (Å)	22.3306(18)	23.6972(11)
α (°)	90	90
β (°)	96.2060(10)	99.9680(10)
γ (°)	90	90
V (Å ³)	4489.6(6)	4868.8(4)
Space group	P2 ₁ /c	P2 ₁ /n
Z	4	4
D _{calcd} (g/cm ³)	1.315	1.272
μ(cm ⁻¹)	5.28	4.90
R1, wR2 (I>2σ(I)) ^a	0.0439, 0.0648	0.0401, 0.0669

Table 5.1. (cont.)

[PhBP ₃]CoCl ₂ (5.9)	
Chemical formula	C ₄₅ H ₄₂ BCl ₂ P ₃ Co · 2 (C ₆ H ₆)
Formula weight	971.54
T (°C)	-177
λ (Å)	0.71073
a (Å)	10.8683(12)
b (Å)	13.3303(14)
c (Å)	16.8858(18)
α (°)	93.356(2)
β (°)	96.607(2)
γ (°)	103.506(2)
V (Å ³)	2353.7(4)
Space group	P $\bar{1}$
Z	2
Dcalcd (g/cm ³)	1.371
μ(cm ⁻¹)	6.20
R1, wR2 (I>2σ(I)) ^a	0.0620, 0.1073

References cited

- 1) a) Groves, J. T.; Takahashi, T. *J. Am. Chem. Soc.* **1983**, *105*, 2073-2074. b) LaPointe, R. E.; Wolczanski, P. T.; Mitchell, J. F. *J. Am. Chem. Soc.* **1986**, *108*, 6382-6384. c) Cummins, C. C. *Chem. Commun.* **1998**, 1777-1786. d) Donahue, J. P.; Lorber, C.; Nordlander, E.; Holm, R. H. *J. Am. Chem. Soc.* **1998**, *120*, 3259-3260. e) Woo, L. K.

-
- Chem. Rev.* **1993**, *93*, 1125-1136. f) Crevier, T. J.; Lovell, S.; Mayer, J. M.; Rheingold, A. L.; Guzei, I. A. *J. Am. Chem. Soc.* **1998**, *120*, 6607-6608.
- 2) a) Mansuy, D.; Mahy, J.; Dureault, A.; Bedi, G.; Battioni, P. *J. Chem. Soc., Chem. Commun.* **1984**, 1161-1163. b) Li, Z.; Conser, K. R.; Jacobsen, E. N. *J. Am. Chem. Soc.* **1993**, *115*, 5326-5327. c) Evans, D. A.; Faul, M. M.; Bilodeau, M. T. *J. Am. Chem. Soc.* **1994**, *116*, 2742-2743. d) DuBois, J.; Tomooka, C. S.; Hong, J.; Carreira, E. M. *Acc. Chem. Res.* **1997**, *30*, 364-372.
- 3) a) Tshuva, E. Y.; Lee, D.; Bu, W.; Lippard, S. J. *J. Am. Chem. Soc.* **2002**, *124*, 2416-2417. b) Solomon, E. I.; Brunold, T. C.; Davis, M. I.; Kemsley, J. N.; Lee, S. K.; Lehnert, N.; Neese, F.; Skulan, A. J.; Yang, Y.; Zhou, J. *Chem. Rev.* **2000**, *100*, 235-249. c) Meunier, B. *Biomimetic Oxidations Catalyzed by Transition Metal Complexes*; Imperial College Press: London, 2000. d) Holm, R. H. *Coord. Chem. Rev.* **1990**, *100*, 183-221. e) Matsunaga, P. T.; Hillhouse, G. L.; Rheingold, A. L. *J. Am. Chem. Soc.* **1993**, *115*, 2075-2077. f) Fischer, B.; Enemark, J. H.; Basu, P. J. *Inorg. Biochem.* **1998**, *72*, 13-21. g) Liang, H. C.; Dahan, M.; Karlin, K. D. *Curr. Opin. Chem. Biol.* **1999**, *3*, 168-175.
- 4) a) Wigley, D. *Prog. Inorg. Chem.* **1994**, *42*, 239-482. b) Nugent, W. A.; Mayer, J. M. *Metal-Ligand Multiple Bonds*; John Wiley and Sons: New York, 1988. c) Thyagarajan, S.; Incarvito, C. D.; Rheingold, A. L.; Theopold, K. H. *Chem. Commun.* **2001**, 2198-2199. d) Lange, S. J.; Miyake, H.; Que, L., Jr. *J. Am. Chem. Soc.* **1999**, *121*, 6330-6331. e) Wang, D.; Squires, R. R. *J. Am. Chem. Soc.* **1987**, *109*, 7557-7558.

-
- 5) a) Glueck, D. S.; Wu, J.; Hollander, F. J.; Bergman, R. G. *J. Am. Chem. Soc.* **1991**, *113*, 2041-2054. b) Glueck, D. S.; Hollander, F. J.; Bergman, R. G. *J. Am. Chem. Soc.* **1989**, *111*, 2719-2721.
- 6) Hay-Motherwell, R. S.; Wilkinson, G.; Hussain-Bates, B.; Hursthouse, M. B. *Polyhedron* **1993**, *12*, 2009-2012.
- 7) a) Betley, T. A.; Peters, J. C. *J. Am. Chem. Soc.* **2004**, *126*, 6252-6254. b) Ruhde, J. U.; In, J.; Lim, M. H.; Brennessel, W. W.; Bukowski, M. R.; Stubna, A.; Münck, E.; Nam, W.; Que, L., Jr. *Science* **2003**, *299*, 1037-1039 c) MacBeth, C. E.; Golombek, A. P.; Young, V. G., Jr.; Yang, C.; Kuczera, K.; Hendrich, M. P.; Borovik, A. S. *Science* **2000**, *289*, 938-941.
- 8) Verma, A. K.; Nazif, T. N.; Achim, C.; Lee, S. C. *J. Am. Chem. Soc.* **2000**, *122*, 11013-11014.
- 9) Brown, S. D.; Betley, T. A.; Peters, J. C. *J. Am. Chem. Soc.* **2003**, *125*, 322-323.
- 10) Betley, T. A.; Peters, J. C. *J. Am. Chem. Soc.* **2003**, *125*, 10782-10783.
- 11) Jenkins, D. M.; Betley, T. A.; Peters, J. C. *J. Am. Chem. Soc.* **2002**, *124*, 11238-11239.
- 12) Dai, X.; Kapoor, P.; Warren, T. H. *J. Am. Chem. Soc.* **2004**, *126*, 4798-4799.
- 13) Hu, X.; Meyer, K. *J. Am. Chem. Soc.* **2004**, *126*, 16322-16323.
- 14) Mindiola, D. J.; Hillhouse, G. L. *J. Am. Chem. Soc.* **2001**, *123*, 4623-4624.
- 15) Mindiola, D. J.; Hillhouse, G. L. *Chem. Commun.* **2002**, 1840-1841.
- 16) Waterman, R.; Hillhouse, G. L. *J. Am. Chem. Soc.* **2003**, *125*, 13350-13351.
- 17) See Chapters 2 and 3 as well as: a) Shapiro, I. R.; Jenkins, D. M.; Thomas, J. C.; Day, M. W.; Peters, J. C. *Chem. Commun.* **2001**, 2152-2153. b) Jenkins, D. M.; Di Bilio,

-
- A. J.; Allen, M. J.; Betley, T. A.; Peters, J. C. *J. Am. Chem. Soc.* **2002**, *124*, 15336-15350.
- 18) Glueck, D. S.; Green, J. C.; Michelman, R. I.; Wright, I. A. *Organometallics* **1992**, *11*, 4221-4225.
- 19) Heinze, K.; Huttner, G.; Zsolnai, L.; Schober, P. *Inorg. Chem.* **1997**, *36*, 5457-5469.
- 20) de Carvalho, L. C. A.; Dartiguenave, M.; Dartiguenave, Y.; Beauchamp, A. L. *J. Am. Chem. Soc.* **1984**, *106*, 6848-6849.
- 21) Ghilardi, C. A.; Mealli, C.; Midollini, S.; Orlandini, A. *Inorg. Chem.* **1985**, *24*, 164-168.
- 22) a) Sacconi, L. *Coord. Chem. Rev.* **1972**, *8*, 351-367. b) Morassi, R.; Bertini, I.; Sacconi, L. *Coord. Chem. Rev.* **1973**, *11*, 343-402.
- 23) Bencini, A.; Gatteschi, D. *Trans. Metal Chem.* **1982**, *8*, 97-119.
- 24) Brown, S. D.; Peters, J. C. *J. Am. Chem. Soc.*, *accepted*.
- 25) a) Li, Z.; Quan, R. W.; Jacobsen, E. N. *J. Am. Chem. Soc.* **1995**, *117*, 5889-5890. b) Omura, K.; Murakami, M.; Uchida, T.; Irie, R.; Katsuki, T. *Chem. Lett.* **2003**, *32*, 354-355.
- 26) a) Dauban, P.; Dodd, R. H. *Synlett* **2003**, *105*, 1571-1586. b) O'Conner, K. J.; Wey, S.; Burrows, C. J. *Tetrahedron Lett.* **1992**, *33*, 1001-1004.
- 27) Brown, S. D.; Peters, J. C. *J. Am. Chem. Soc.* **2004**, *126*, 4538-4539.
- 28) Warren, K. D. *Struct. and Bond.* **1976**, *27*, 45-159.
- 29) A platinum terminal oxo complex has recently been reported. See: Anderson, T. M.; Neiwert, W. A.; Kirk, M. L.; Piccoli, P. M. B.; Schultz, A. J.; Koetzle, T. F.; Musaev, D. G.; Morokuma, K.; Cao, R.; Hill, C. L. *Science* **2004**, *306*, 2074-2077. Two points

-
- are worth mentioning about this complex. First, the authors do not characterize it as a metal-ligand multiple bond based on their molecular orbital diagram. They claim it is only a Pt-O single bond. Second, the metal cluster nature of the ligands may stabilize the supposed d^6 configuration by delocalizing electron density away from the Pt center to the ligands.
- 30) Based on this hypothesis, it should be possible to synthesize a terminal Co(III) d^6 oxo in a trigonal planar geometry given that Hillhouse has prepared a trigonal planar d^8 imide. Warren and co-workers have made the bridged bis- μ_2 -oxo instead of a terminal oxo using the same auxiliary ligands that stabilized a terminal imide. This is not surprising given that the bridged oxo may be thermodynamically more stable.
- 31) See Chapter 4 for synthesis and discussion of $\{[\text{PhBP}_3]\text{CoOSiPh}_3\} \{\text{BAr}_4\}$ (Ar = Ph or 3,5-(CF₃)₂-C₆H₃).
- 32) To try to limit the effects of sterics in protecting the terminal imide, it would be of interest to see if an imido complex with a methyl group off of the nitrogen such as $[\text{PhBP}_3]\text{CoNMe}$ is stable. The $[\text{PhBP}_3]\text{Co}$ system so far has not proven to be sterically effected by smaller R groups unlike the Hillhouse, Meyer, Bergman, and Warren systems that either degrade or form bridging imides.
- 33) Currently only 17 terminal $\text{M}\equiv\text{NH}$ species have been reported (CCDC search, 2005). This is two orders of magnitude below the number of $\text{M}\equiv\text{NR}$ species reported.
- 34) For a d^3 $\text{M}\equiv\text{NH}$ species see: a) Huynh, M. H.; White, P. S.; John, K. D.; Meyer, T. J. *Angew. Chem., Int. Ed. Engl.* **2001**, *40*, 4049-4051. For d^2 examples see: b) Hagenbach, A.; Strahle, J. Z. *Anorg. Allg. Chem.* **2000**, *626*, 1613-1619. c) Yoshida, T.; Adachi, T.; Yabunouchi, N.; Ueda, T.; Okamoto, S. *Chem. Commun.* **1994**,

-
- 151-152. d) Ishino, H.; Tokunaga, S.; Seino, H.; Ishii, Y.; Hidai, M. *Inorg. Chem.* **1999**, *38*, 2489-2496.
- 35) Jaguar 5.0, Schrodinger, LLC, Portland, Oregon, 2002.
- 36) Becke, A. D. *J. Chem. Phys.* **1993**, *98*, 5648-5652.
- 37) Lee, C.; Yang, W.; Parr R. G. *Phys. Rev. B* **1988**, *37*, 785-789.
- 38) Smith, P. A. S.; Brown, B. B. *J. Am. Chem. Soc.* **1951**, *73*, 2438-2441.
- 39) Abramovitch, R. A.; Challand, S. R.; Scriven, E. F. V. *J. Org. Chem.* **1972**, *37*, 2705-2710.
- 40) a) Li, Y.; Kirby, J. P.; George, M. W.; Poliakoff, M.; Schuster, G. B. *J. Am. Chem. Soc.* **1988**, *110*, 8092-8098. b) Smith, P. A. S.; Hall, J. H. *J. Am. Chem. Soc.* **1962**, *84*, 480-485.
- 41) Bottaro, J. C.; Penwell, P. E.; Schmitt, R. J. *Syn. Comm.* **1997**, *27*, 1465-1467.